Road Infrastructure Mapping by Using iPhone 14 Pro: An Accuracy Assessment

B. Suleymanoglu[1], R. Tamimi[2], Y. Yilmaz[1], M. Soycan[1], C. Toth[2]

[1]Civil Engineering Faculty, Yildiz Technical University, 34220 Esenler Istanbul, Turkey – (bariss, soycan, yilmazy)@yildiz.edu.tr
[2]SPIN Laboratory, Department of Civil, Environmental and Geodetic Engineering, The Ohio State University,
470 Hitchcock Hall, 2070 Neil Ave., Columbus, OH 43210 – (tamimi.12, toth.2)@osu.edu

KEY WORDS: LiDAR, photogrammetry, point cloud analysis, feature detection, smart devices, GNSS RTK

ABSTRACT:

Vital aspects of transportation networks, such as the extraction of road information and analysis of road conditions, have become increasingly important research topics as they outline the foundation of many applications such as high-precision mapping, infrastructure planning and maintenance, intelligent transportation, or road design analysis. Therefore, regularly obtaining accurate high-density point cloud data of infrastructures supports many transportation-based applications and provides up-to-date information for smart cities or digital twins. Low-cost smartphone platforms equipped with a variety of sensors provide new and powerful data acquisition capabilities that can be exploited in the geospatial field. For example, mobile phones are now capable of collecting valuable data to generate accurate models to support digital reconstruction of infrastructures. These platforms can provide simple and effective data acquisition, while offering useful geospatial data that can be an alternative to traditional measurement techniques. However, the sensor performance with respect to spatial accuracy of point clouds generated in different applications have not yet been fully investigated. Thus, this paper evaluates the feasibility of using the point clouds generated by the built-in camera and LiDAR sensors integrated into iPhone 14 Pro for extracting road-related information. Additionally, the use of the viDoc RTK Rover on the iPhone 14 Pro increases the platform positioning accuracy, consequently improving the georeferencing accuracy of the point clouds. To validate the performance of the point clouds obtained by the iPhone 14 Pro, a reference dataset of the road features was obtained by measuring with a single-point RTK-GNSS receiver, receiving corrections from the Turkish CORS network (TUSAGA-Aktif) which provides two to three centimetres of accuracy. In addition, reference point cloud data over the same area was obtained from different platforms such as Mobile LiDAR and UAS, and the road features were extracted from these dataset and performance validated. The data acquired by the iPhone 14 Pro was processed and evaluated with respect to the reference datasets. The advantages and disadvantages of using iPhone 14 Pro are analysed in detail and the findings are reported.

1. INTRODUCTION

The extraction of road information from high accuracy point clouds has become an important tool in the geospatial field in recent years, thanks to the development of a variety of sensors that provide powerful data acquisition capabilities. Some of these methods include Mobile Mapping Systems on vehicles like automobiles or aircrafts to collect data with sensors to generate point clouds. Point clouds are three-dimensional data sets that consist of many points in space, each of which has a set of coordinates and frequently other attributes such as colour or intensity. Point clouds can be generated using a variety of sensors, including lasers and cameras. The use of the LiDAR (Light Detection and Ranging) sensor significantly improves point cloud creation by capturing more points in areas where camera sensors may struggle to see, as well as the speed at which they can be collected. Using a camera sensor, images can be taken at a set interval and stitched together utilizing photogrammetry to reconstruct the entire site. The accuracy of data collected could be improved with the use of RTK corrections, which would be essential for point clouds generated , as VRS provides the best solution currently(Puente, I., et al. 2013).

Smartphones offer a convenient and accessible means of data acquisition for various mapping applications, including road infrastructure mapping. With the advancements in sensors and technologies, such as the integration of LiDAR and RTK systems, mobile phones can provide accurate and precise data for mapping applications, making them potentially a useful and efficient tool for road infrastructure mapping.
Early testing of the iPhone shows the framework of research that indicated the potential use of mobile phones for collecting data for mapping purposes. (Sirmacek, B. et al. 2014) conducted a study to assess the accuracy of building point clouds generated from iPhone 3GS's images. They used the iPhone's camera sensor to capture images of building facades, and then used specialized software to process the images and generate point clouds. The accuracy of the building point clouds generated from the iPhone images was compared to the reference point clouds obtained using a total station, a precision surveying instrument. The results showed that the building point clouds had an average accuracy of 3-5 cm, with a maximum error of 15 cm. The authors also analysed the distribution of the errors and found that most of the errors were concentrated near the edges of the building facades, where the texture and features were more complex. The accuracy of the point clouds generated from iPhone images was concluded to be sufficient for many mapping applications, and that the technology had the potential to be a useful tool for quickly and efficiently generating building point clouds in the future.

More recent studies with iPhones include a LiDAR sensor. (Luetzenburg. et al. 2021) carried out a series of experiments to evaluate the performance of the iPhone 12 Pro LiDAR for engineering applications. They used the iPhone to measure a range of objects, including trees, buildings, and terrain, and compared the results to those obtained using other LiDAR systems. The authors found that the iPhone was able to provide accurate and precise measurements for these objects, with an average accuracy of 0.5-1.5 cm and an average precision of 0.2-0.5 cm. The iPhone performed particularly well when measuring flat surfaces and objects with clear features, such as buildings and trees. However, it performed less well when measuring objects with complex shapes or rough surfaces, such as rocks and terrain.

This case study investigates the feasibility of using a mobile phone like the iPhone 14 Pro with its integrated camera and LiDAR sensor, along with a viDoc RTK Rover to capture data to generate a point cloud and assess the accuracy for road infrastructure mapping. LiDAR-based systems have been extensively utilized in road-related applications, including the extraction of geometric characteristics, road surface analysis, traffic sign detection, and inventory mapping, as demonstrated in previous literature (Gargoum and El-Basyouny 2017; Ma et al., 2018;). The present study aimed to compare the advantages and disadvantages of iPhone 14 Pro data with respect to the commonly used mobile LiDAR and unmanned aerial vehicle (UAV) LiDAR in such applications. The study area was previously surveyed and mapped using a GNSS receiver with a Virtual References System (VRS) on the Turkish Continuously Operating Reference System (CORS) network (TUSAGA-Aktif) to generate a reference dataset for result comparison. The purpose of this paper is to evaluate the performance and accuracy of the mobile phone geospatial sensor technology, including performance validation in a controlled environment. This will provide insight into the capabilities of using an iPhone 14 Pro and viDoc RTK Rover for road infrastructure mapping, and how it compares to traditional methods.

2. MATERIALS AND METHODS

2.1 Study Areas, Data Acquisition Systems and Datasets

2.1.1 iPhone 14 Pro + viDoc RTK Rover

The viDoc RTK Rover was an essential component of the mapping process, providing real-time kinematic (RTK) positioning to improve the accuracy of the mapping results with respect to the stock GNSS receiver built in the iPhone. The CORS stations continuously monitor signals from satellites and transmit RTK correction signals to the viDoc RTK Rover, which uses this information to provide centimetre-level accuracy positioning. The viDoc RTK Rover was connected to the iPhone 14 Pro via Bluetooth, allowing the iPhone 14 Pro to receive real-time corrections, and improve the positioning of the system. The iPhone 14 Pro was equipped with a high-resolution camera and LiDAR (light detection and ranging) sensor, which were used to capture imagery and depth data, respectively. The camera captured images of the road infrastructure, while the LiDAR sensor generated a point cloud of the area, providing a comprehensive 3D representation of the object space that allows us to interpret road infrastructure. The Pix4Dcatch app was utilized for image processing and automatic alignment between the images and LiDAR data, improving the accuracy and efficiency of the mapping process. The Pix4Dcatch app was used to process the data collected by the iPhone 14 Pro and RTK Rover to create a 3D reconstruction of the road infrastructure. The app automatically aligned the images and LiDAR and used the RTK data to improve the geolocation accuracy of the mapping results. The Bluetooth connectivity between the iPhone 14 Pro and the RTK Rover allowed for real-time corrections to be received by the iPhone 14 Pro, further improving the accuracy of the mapping results.

2.1.2 UAV-LiDAR

Another survey of the study area was performed using a UAV-LiDAR system. The specific system used in this study was the Phoenix Alpha-32 LiDAR system (see Figure 1). The system consisted of several components, including a Velodyne laser scanner, a high-precision inertial measurement unit (IMU) from OEM-ADIS16488, NovAtel OEM6 dual-frequency GNSS receivers and a microcomputer.

Figure 1. UAV-LiDAR System (Phoneix, 2023)

2.1.3 Mobile LiDAR

Another measurement system used in the study area was a Mobile LiDAR system. The system consisted of several components, including a Velodyne laser scanner, a Ladybug5 camera, two dual-frequency GNSS receivers a high-precision inertial measurement unit (IMU), and an odometer (refer to Figure 2).

Figure 2. Mobile LiDAR System (AnkaGeo, 2023)

2.1.4 Study Areas and Datasets

The experiment took place on the Davutpasa Campus of Yildiz Technical University in Istanbul. The study area was a 90-meter-long and 7-meter-wide corridor with a 5.5% slope, as shown in Figure 3. This corridor is a two-lane road that includes a change in slope both across and along the road, as well as sidewalks.

(a) (b)

Figure 3. Study Area:
3D view of the point cloud (a), 2D image (b)

2.2 Methodology

2.2.1 Point Cloud Generation

The combination of the iPhone 14 Pro and the Pix4Dcatch app allowed for real-time data collection and processing of the LIDAR point cloud data in the field. The Pix4Dcatch app processed the data from the LiDAR sensor to generate a point cloud. To improve the geolocation accuracy of the mapping results, it also utilized data from the viDoc RTK rover received via the VRS network. The LiDAR point cloud data captured by the Pix4Dcatch app on the iPhone 14 Pro provided a preliminary representation of the point cloud, but further processing of the images was required to create a high-resolution point cloud by providing more data captured by the camera sensor. The data collected on the iPhone 14 Pro was then transferred to the Pix4Dmatic software on a computer for further processing. The Pix4Dmatic software utilized the LIDAR point cloud data in combination with the imagery data captured by the iPhone 14 Pro by fusing both point clouds to generate a more detailed and accurate representation of the road infrastructure. The software also employed advanced algorithms and computer vision techniques to further improve the accuracy of the mapping results. Besides using RTK GNSS data, the Pix4Dmatic software incorporated georeferencing data, control points gathered by a GNSS receiver in the field. This data was used to reference the positions in the point cloud that were marked and easily identifiable by the user. Photogrammetric image processing used in Pix4Dmatic allowed for the creation of a highly detailed and accurate 3D representation of the object space. The software automatically aligned the LIDAR point cloud data and imagery data and used the RTK GNSS data and georeferencing data to improve the accuracy of the mapping results. .

2.2.2 Accuracy Assessment of Point Cloud

The absolute accuracy of the point cloud data was assessed by comparing manually measured RTK-GNSS ground control points (GCPs) with digital elevation models (DEMs) created from the point cloud data. Point clouds generated by systems, such as UAV-Lidar, MLS, and iPhone, needs some common reference from to perform comparisons. Here we used a regular DEM for our evaluation and
selected interpolation method of inverse distance weighting (IDW), which is widely used for interpolating irregularly spaced data sets, such as point clouds (Shams et al., 2018; Barbarella et al., 2019). The optimal grid resolution for this study was determined using Equation 1, which was suggested by Hengl (2006) and it can accurately calculate the minimum grid resolution (p) based on the data density. Different DEM surfaces were generated at various grid resolution calculations for each dataset.

$$p = 0.5 * \sqrt{\frac{1}{D}} \quad (1)$$

where D is the average point density (number of point/dm^2)

The elevation difference was calculated between each RTK-GNSS GCP (Z_{GCP}) and the elevation of the point at the same position (Z_{DEM}) in DEM. Furthermore, the root mean square error (RMSE) and standard deviation (SD were computed by utilizing the vertical discrepancies between the observed RTK-GNSS control points (Z_{GCP}) and the points on the DEM surface at corresponding positions (Smith et al., 2014, Tamminga et al., 2015). These points are independent of the point cloud and DEM generation and spaced throughout the study area. Figure 4. illustrates the study area's as shaded relief DEM, derived from point cloud data along with the spatial distribution of 170 ground control points. The RMSE and SD were calculated as follows:

$$\text{Root-Mean-Square-Error } (RMSE) = \sqrt{\frac{\sum_{i=1}^{n}(Z_{GCP(X_i-Y_i)})^{-Z_{DEM(X_i-Y_i)}}}{n}} \quad (2)$$

$$\text{Standard Deviation } (SD) = \sqrt{\frac{\sum_{i=1}^{n}\left(\left(Z_{GCP(X_i-Y_i)}\right)^{-Z_{DEM(X_i-Y_i)}}\right)-\mu)}{n-1}} \quad (3)$$

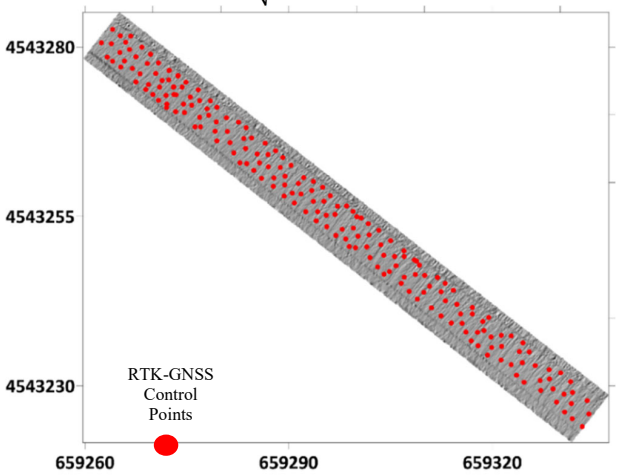

Figure 4. Example of shaded relief map of DEM where red dots shows distribution of RTK-GNSS ground control points

2.2.3 Trajectory based Partitioning and Road Edge Detection

To reduce processing time and increase the accuracy of the road infrastructure assessment, the images captured by the iPhone 14 Pro's camera sensor position at each measurement point during the test run was used as trajectory data. The point cloud data was partitioned perpendicular to the trajectory data from the iPhone using a predefined length. Subsequently, numerous cross sections were formed from each data block with a predefined width. Each cross section thus contains data belonging to the road surface, curbs, sidewalks, and various objects including trees, traffic lights, and vehicles. As seen in Figure 5(a), the study area is divided into rectangular blocks, and cross-sections extracted from each block are projected perpendicular to the plane, as shown in Figure 5(b). The red dots indicate the trajectory data for iPhone 14 Pro camera sensor. Since all three datasets were obtained from the same area, the same trajectory data was also used to divide the MLS and UAV-LiDAR data into blocks.

Based on the extracted cross-sections from each data block, curb points were determined from the raw point cloud data using our proposed methodology, which is based on the slope and elevation difference parameters. In general, road surfaces consist of smooth surfaces with low slope and height differences, and there are serious variations in slope and height in the transition to sidewalks. However, as there are points belonging to different objects (such as trees and streetlights) in each section, these points must first be identified and removed from the dataset. Therefore, the detection and filtering of these points were performed using the elevation difference in each cross-section. For this, the elevation difference between points with maximum and minimum height was calculated and compared with the height of the curb in the study area. The point is classified as an object point if its elevation differences are higher than the curb

elevation. This iterative process continued until there were no more points than the curb height in each cross-section.

$$\Delta Z_i = \max(Z_i) - \min(Z_i)$$
$$\text{if } Z_{curb} < \Delta Z_i \rightarrow \text{object points} \quad (4)$$
$$\text{otherwise } p_i \text{non-object points}$$

Where, ΔZ_i maximum elevation difference, curb height, which is 20 cm in the study area. After detecting the object points, our slope-based methodology was applied to detect curb points. Thus, the search algorithm was implemented from the scan centre to two different directions in each cross-section, and slope values were calculated between consecutive points using the formulas in equation 5. As stated above, the elevation of the pavement points is higher than the road surfaces, and in general, there are abrupt slope changes in the transition from road surfaces to sidewalks. Accordingly, the curb points were determined by comparing the calculated slope values with the threshold value.

$$Sp_i^{i+1} = \frac{Z_{i+1} - Z_i}{\sqrt{(X_{i+1} - X_i)^2 - (Y_{i+1} - Y_i)^2}} \quad (5)$$

Where, $(X_{i+1,i}, Y_{i+1,i}, Z_{i+1,i})$ express the coordinate values of consecutive points, Sp_i^{i+1} denote calculated slope values. If the calculated slope value is greater than the predetermined slope threshold value ($S_{threshold}$), it is classified as a curb point.

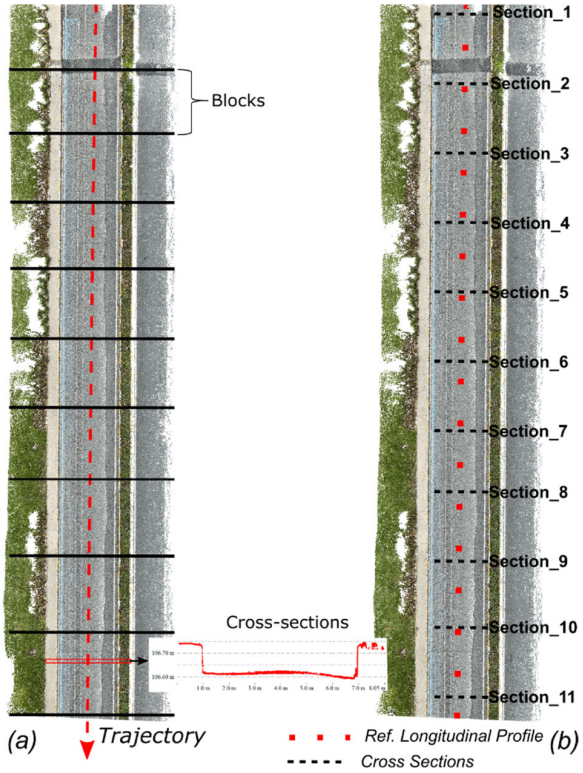

Figure 5, a) Splitting the study area into rectangular blocks and forming cross-sections, b) red dots show reference longitudinal profile points in the study area, black dashed lines indicate reference cross-sections.

Following the detection of candidate curb points, the road boundaries were segmented into left and right road boundaries based on trajectory information. Subsequently, falsely detected curb points were identified and eliminated through the implementation of the RANSAC algorithm (Fischler and Bolles, 1981). This methodology enabled the removal of erroneous data points and improved the accuracy of the curb detection process. Consequently, the boundaries of the road were extracted using detected curb points with the polynomial curve fitting method.

2.2.4 Extraction and Comparison of Road Geometry Parameters (road width, road centerline, Longitudinal Profile and if possible cross-slope)

The data obtained from the previous step, which involved determining the road surface and boundaries, was utilized to determine the geometric parameters of the road. Thus, many important geometric parameters such as road width, elevation, and slope for longitudinal and cross-sectional profiles of the road surface were calculated quickly and accurately together with the road centreline.

The methodology proposed by Yadav et al. (2018) was employed to determine the road width and road centreline. Firstly, refined curb points identified in the previous section were selected and segmented by sequentially aligning them along the road boundary. Next, a polynomial line was fitted to the points within this segment, and the slope values (s_i) of the line were calculated. The slope of the perpendicular line (s_j) with respect to this line was determined using equation 6. Lastly, the points on the other side of the road boundary were substituted into equation7, and the points with the minimum residuals were chosen (Yadav et al., 2018).

$$s_i * s_j = -1 \quad (6)$$
$$y - y_1 = s_j * (x - x_1) \quad (7)$$

As mentioned earlier, one of the significant geometric parameters that were obtained is the longitudinal profile information. To obtain this information, the planimetric coordinates and height values of the reference longitudinal profile points were measured using the RTK-GNSS technique, with intervals of approximately 8 meters on average as seen in Figure 5(b). To compare the reference longitudinal data with point clouds data obtained by MLS, UAV-LiDAR and iPhone-viDoc RTK, the points closest to the reference longitudinal points within these point clouds were determined using a k-nearest neighbour search (k is selected as 1).

The following step involved identifying eleven transverse sections along the road line, as shown in Figure 5(b), and measuring and calculating the cross-slope values of these sections. To evaluate performance accuracy, the cross-slope values derived from the point clouds were compared to the reference cross-slope values of the identified sections. The reference cross-slope values were calculated by measuring the pavement points or lane lines using the RTK-GNSS technique providing 2-3 centimetre accuracy (Badescu et al.,2011; Garrido et al.,2011).. The cross-slope value was obtained by applying linear regression to the extracted data of the point clouds within specified cross-sections, and the cross-slope values were determined as the slope of the regression line. All the procedures were implemented in the MATLAB environment.

3. RESULTS

3.1 Accuracy Assessment of Point Clouds

Absolute accuracy was evaluated based on manually measured RTK-GNSS measurements. The calculated error statistics for DEM surfaces with respect to each RTK-GNSS point are given

in table 1. As seen in the table, all statistical values are below the centimetre level. Upon analysing the error statistics of both systems, it was determined that the point cloud data obtained from all systems exhibited minimal discrepancies. Furthermore, the results indicated that the vertical accuracy of all point cloud data was notably high, and the datasets were georeferenced with satisfactory precision at the centimetre scale, which was deemed suitable for the purpose of this study.

	Min (m)	Max (m)	STN (m)	RMSE (m)
UAV-LiDAR	-0.03	0.10	0.02	0.03
MLS	-0.05	0.10	0.03	0.03
iPhone-viDoc	-0.06	0.01	0.02	0.04

Table 1. Error statistics for point cloud data

Figure 6 presents a comparative analysis of longitudinal profiles between the reference data and the data derived from UAV-LiDAR, MLS, and iPhone-viDoc. The dashed black line, blue circle, and orange crosshair indicate the height differences between the reference longitudinal profiles and those derived from UAV-LiDAR, MLS, and iPhone-viDoc, respectively. Statistical values for these height differences are given in Table 2. Upon examining the height differences obtained from all three systems, deviations were observed in certain areas. However, further investigation revealed that the error values remained within the centimetre level, indicating highly consistent results across all three systems. In addition, the variances of the height differences are slightly higher with MLS and UAV-LiDAR, compared to the iPhone. As a result, the georeferencing of iPhone data may exhibit greater consistency in this regard.

Reference Profiles Comparison	Min (m)	Max (m)	STN (m)	RMSE (m)
UAV-LiDAR	-0.03	0.02	0.01	0.01
MLS	-0.04	0.02	0.02	0.02
iPhone-viDoc	-0.02	-0.01	0.01	0.01

Table 2. Error statistics values of longitudinal profile differences

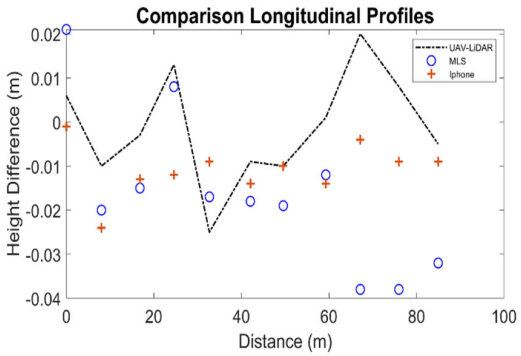

Figure 6. Comparison of different longitudinal profiles: UAV-LiDAR, MLS, and iPhone

The result of our road boundary extraction is depicted as a set of red points and a vectorized road boundary represented by a green line. These representations have been overlaid onto the point clouds obtained from unmanned aerial vehicles (UAVs), mobile laser scanning (MLS), and iPhone sources, respectively, as presented in Figure 7.

We visually inspected several parts of typical road scenes that have been enlarged using our method. The road boundaries are generally extracted correctly, but there may be instances where our method fails to draw boundaries due to the nature of the point cloud data or because of differences in pavement structures. Thus, as illustrated in Figure 7 (c, d), it has been determined that road boundaries are unable to be extracted due to insufficient data on the curb points using the UAV LiDAR system in those road sections. To alleviate the limitations of this system, several scans should be acquired from different viewpoints to generate comprehensive point clouds of a scene. As shown in Figure 7 (g-k-l), deviations from the curb boundary were observed in certain sections due to the incorrect detection of some points as pavement points from MLS and iPhone-based point clouds. Both systems have the ability to acquire a more comprehensive and complete representation of the road surface, primarily due to sensors scanning angles and positions. This feature ensures that the proposed methodology is capable of obtaining appropriate data. However, it should be noted that the scanning capacity of the iPhone is restricted to shorter routes, limiting its application in certain scenarios.

In addition, the average road width was calculated from the obtained refined boundary points. The calculated road width values were compared with field measurements to determine any deviations from the reference values. The results indicated that the road width values obtained from MLS, UAV-LiDAR, and iPhone deviated from the reference values by 2.7%, 0.5%, and 3.4%, respectively. Additionally, The UAV-LiDAR performed better than the MLS and the iPhone because, as shown in figure 7, both systems had faulty boundaries detected in some parts of the road.

In the Table 3, reference cross-slope values were determined using RTK-GNSS data and subsequently compared against values obtained from UAV-LiDAR, MLS, and iPhone. The cross-slope difference between reference and UAV-LiDAR ranged from 0.01% to 0.65%, with an average difference of 0.25%. Similarly, the difference between reference and MLS cross-slope values ranged from 0.03% to 0.44%, with an average difference of 0.20%. For the iPhone, the cross-slope difference ranged from 0.02% to 0.69%, with an average difference of 0.19%. The acceptable accuracy for cross-slope differences, as defined by relevant literature and technical guidelines, is generally considered to be 0.2% (Shams et al.,2018; Hunt et al., 2013). Based on the obtained results, it can be concluded that the average difference values obtained by all three methods were close to this acceptable limit. Therefore, the systems evaluated in this study show promising results for cross-slope evaluation.

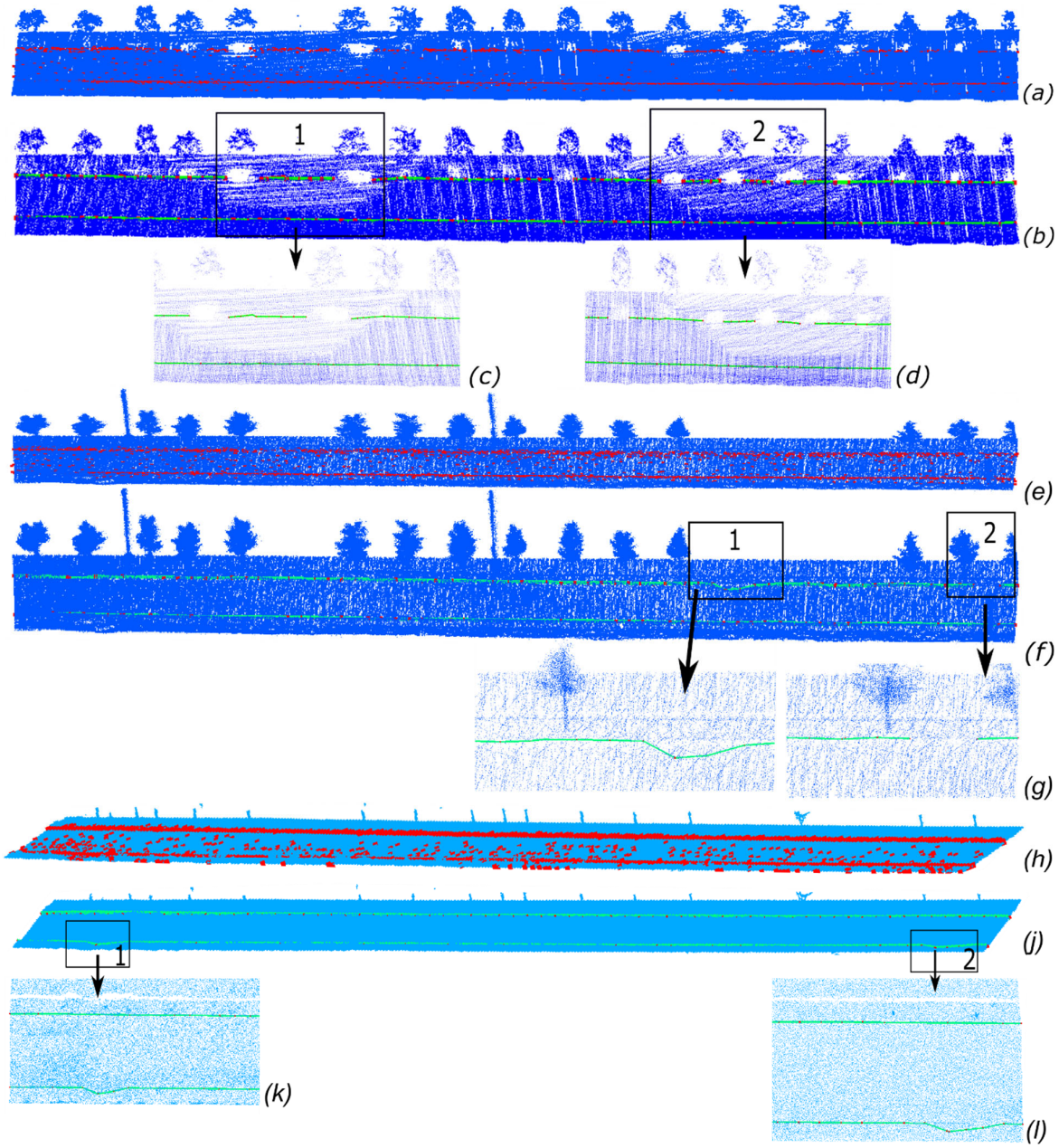

Figure 7: Road boundary extraction results for UAV-LiDAR (a-b-c-d), MLS (e-f-g), and iPhone (h-j-k-l). (a-e-h) shows the initially detected curb points, (b-f-j) shows the refined curb points (in red), and the vectorized road boundary is shown in green. Enlarged images in (c-d-g-k-l) show missing road parts and false curb boundaries.

4. DISCUSSION AND CONCLUSIONS

The study aimed to evaluate the accuracy of road infrastructure mapping and cross-slope evaluation using an iPhone 14 Pro with the viDoc RTK Rover. The absolute accuracy of the point cloud data was evaluated based on manual measurements taken from a GNSS receiver. The iPhone-viDoc point cloud was also compared to MLS and UAV-LiDAR data obtained in the same study area. The results indicate that the vertical accuracy of the iPhone-viDoc point cloud data was noticeably higher, with error values around the centimetre level. The dataset was georeferenced with satisfactory precision at the centimetre scale. This suggests that all three methods can be used for road boundary extraction and cross-slope evaluation with a high level of accuracy.

The road boundary extraction results for all three systems indicated that road boundaries were generally extracted correctly. However, there were instances where the method failed to draw boundaries due to the nature of the point cloud data or differences in pavement structures. Deviations from the curb boundary were also observed in certain sections due to the incorrect detection of some points as pavement points from MLS and iPhone-based point clouds. The longitudinal profiles derived from all three systems showed highly consistent results with deviation values within the centimetre level.

		Differences at Ground Truth		
Sec.	**Ground Truth (%)**	**UAV LiDAR (%)**	**MLS (%)**	**iPhone (%)**
1	0.74	0.04	0.34	0.69
2	0.02	0.10	0.12	0.17
3	0.29	0.58	0.29	0.22
4	0.27	0.65	0.27	0.02
5	0.31	0.19	0.13	0.09
6	0.23	0.26	0.03	0.12
7	0.40	0.17	0.09	0.00
8	1.01	0.31	0.44	0.28
9	0.85	0.16	0.33	0.19
10	0.04	0.01	0.10	0.04
11	0.25	0.25	0.10	0.30
Mean		**0.25**	**0.20**	**0.19**

Table 3. Cross-slope comparison between ground truth and UAV-LiDAR, MLS, and iPhone

The cross-slope evaluation results indicate that the average difference values obtained by all three methods were close to the acceptable limit of 0.2%, including the data obtained by the iPhone 14 Pro with the viDoc RTK Rover.

In conclusion, the study demonstrates the potential of using an iPhone 14 Pro with the viDoc RTK Rover for road infrastructure mapping and cross-slope evaluation with high accuracy. The results also show that the iPhone-viDoc point cloud data can be used interchangeably with MLS and UAV-LiDAR data for these purposes. To further improve the experiments, future studies could consider using PPK on the viDoc RAW data to achieve even higher accuracy in georeferencing. Additionally, incorporating machine learning techniques could help improve the road boundary extraction results by automatically identifying and removing pavement points from the point cloud data. The study provides valuable insights for the use of mobile mapping systems in road infrastructure mapping and evaluation.

ACKNOWLEDGEMENT

We would like to express our gratitude to Pix4D for generously supplying us with a viDoc RTK rover, which was instrumental in improving the accuracy of our mapping results. We would also like to thank AnkaGeo for providing us with mobile LiDAR data that was crucial to the success of our project. Without the support and contributions of both companies, this project would not have been possible.

REFERENCES

Shams A., Sarasua W.A., Famili A., Davis W.J., Ogle J.H., Cassule L., Mammadrahimli A. Highway Cross-Slope Measurement using Mobile LiDAR. *Transp. Res. Rec.*, Vol.2(02), 2018, p.p 175-199.

Barbarella M., De Blasiis M.R., Fiani M. Terrestrial laser scanner for the analysis of airport pavement geometry. Int. J. Pavement Eng., Vol.20, No.4, 2019, p.p 466-480.

Hengl T. Finding the right pixel size. Comput. Geosci. Vol.32, No.9, 2006, p.p 1283-1298

Tamminga A.D., Eaton B.C., Hugenholtz C.H. UAS-based remote sensing of fluvial change following an extreme flood event. Earth Surf. Process. Landforms Vol.40, No.11, 2015, p.p 1464-1476.

Smith M.W., Carrivick J.L., Hooke J., Kirkby M.J. Reconstructing flash flood magnitudes using "Structure-from-Motion": A rapid assessment tool. J. Hydrol. Vol.519, 2014, p.p 1914-1927

Fischler, M.A.; Bolles, R.C. Random sample consensus: A paradigm for model fitting with applications to image analysis and automated cartography. Commun. ACM 1981, 24, 381–395.

Yadav, M., Singh, A. K., & Lohani, B. (2018). Computation of road geometry parameters using mobile LiDAR system. Remote Sensing Applications: Society and Environment, 10, 18-23.

Shams A., Sarasua W.A., Famili A., Davis W.J., Ogle J.H., Cassule L., Mammadrahimli A. Highway Cross-Slope Measurement using Mobile LiDAR. *Transp. Res. Rec.*, Vol.2(02), 2018, p.p 175-199.

Hunt J. E., Vandervalk A., and Snyder D. SHRP2 Report S2-S03-RW-01: Roadway Measurement System Evaluation. Transportation Research Board of the National Academies, Washington, D.C., 2013

Phoneix LiDAR Systems. https://www.phoenixlidar.com/wp-content/uploads/2019/11/PLS-AL3-32-Spec-Sheet_180406.pdf, Accessed Time 16/02/2023

Ankageo Geopgrahic Information Technologies. https://ankageo.com/urunler/ Accessed Time 16/02/2023

Badescu, G., Stefan, O., Badescu, R., Ortelecan, M. & Veres, S. I. (2011). Positioning System GPS and RTK VRS Type, Using the Internet as a Base, a Network of Multiple Stations. FIG Working Week 2011, TS03G - GNSS CORS Networks Case Studies (Flash), 5247 / Marrakech, Morocco, 18-22 May 2011

Garrido, M. S., Gimenez, E., Lacy, M. C. & Gil, A. J. (2011). Testing precise positioning using RTK and NRTK corrections provided by MAC and VRS approaches in SE Spain. Journal of Spatial Science, 56(2), 169-184.

Gargoum, S., & El-Basyouny, K. (2017, August). Automated extraction of road features using LiDAR data: A review of LiDAR applications in transportation. In 2017 4th International Conference on Transportation Information and Safety (ICTIS) (pp. 563-574). IEEE.

Ma, L., Li, Y., Li, J., Wang, C., Wang, R., & Chapman, M. A. (2018). Mobile laser scanned point-clouds for road object detection and extraction: A review. Remote Sensing, 10(10), 1531.